

Fig. 2: Enhancing the stability of the 3-generator system along curved paths. **a** Examples of curved paths (red, green, and blue) in the β -space from β_- to β_+ along which the Lyapunov exponent λ^{\max} decreases monotonically. The numerically generated curves confirm our theoretical prediction that these paths are all tangent to the plane L at the point β_- . The droplines indicate that these curves are outside L . The contour levels of λ^{\max} are shown on L . Also shown is the plane M , which is defined as the plane perpendicular to L that contains β_- and β_+ . **b** Contour levels of λ^{\max} on the plane M , which contains the green path from **a**. The orange lines in **a** and **b** indicate the intersection between planes L and M . The red dashed curves (and the green path) trace cusp surfaces associated with degeneracies of the real parts of the eigenvalues of \mathbf{J} that determine λ^{\max} . Three types of degeneracy are indicated: a real eigenvalue equal to the real parts of a pair of complex conjugate eigenvalues ($a, a \pm bi$), two different complex conjugate eigenvalues with equal real parts ($a \pm b_1 i, a \pm b_2 i$), and two equal real eigenvalues (a, a). For details on the system, see Methods.

exist and can connect β_- to the (unique) global minimum, which we denote by β_+ as its components are all different. The corresponding optimal $\lambda^{\max}(\beta_+) \approx -9.41$ represents more than 8% improvement over $\lambda^{\max}(\beta_-) \approx -8.69$. In general, if a curved path starts at β_- , and if λ^{\max} decreases monotonically along that path, then it cannot be oriented in an arbitrary direction in the β -space. We show that it needs to be tangent to a system-specific plane (or hyperplane of co-dimension one for $n > 3$), denoted here by L and defined by the equation $\sum_{i=1}^n u_i v_i \beta_i = 0$, where u_i and v_i are the i th component of the left and right eigenvectors, respectively, associated with the eigenvalue α_2 . This result, illustrated by the three example paths in Fig. 2a, follows from the derivation of a formula for λ^{\max} and the full analytical characterization of the stability landscape near β_- (both presented in [Supplementary Note 1](#)).

The curved paths of decreasing λ^{\max} are part of the complex structure of the stability landscape. These paths generally lie on a cusp surface, defined by the property that, at any point on the surface, λ^{\max} is non-differentiable and locally minimum along any direction transverse to the surface. The three paths shown in Fig. 2a all lie on the same cusp surface, which contains both β_+ and β_- . The intersection between this cusp surface and the plane M (the one perpendicular to L) is the green path of monotonically decreasing λ^{\max} shown in Fig. 2. In fact, there are infinitely many different paths of decreasing λ^{\max} on this cusp surface. Of these paths, the red and blue paths shown in Fig. 2a share the additional property of being an intersection between pairs of cusp surfaces. Each of these paths consists of at least two parts that are intersections between different pairs of cusp surfaces, which explains the kinks observed in Fig. 2 as points at which the curve switches from one intersecting surface to another. In larger systems, we find that their higher-dimensional β -spaces are sectioned by many entangled cusp hypersurfaces associated with spectral degeneracies (as illustrated in Supplementary Fig. 2 using the four larger systems we will introduce below). Their intersections, which themselves form cusp hypersurfaces of lower dimensions, are expected to contain curved paths of monotonically decreasing λ^{\max} . The existence of kinks and cusp surfaces in the stability landscape, which makes numerical search for global optima challenging, is not unique to power grids nor phase oscillator networks. It is a consequence of a much more general mathematical observation that the largest real part of the eigenvalues of a matrix (known as the spectral abscissa), such as λ^{\max} we consider here, is a non-smooth, non-convex, and non-Lipschitz function of the matrix elements²⁶.

Stabilizing heterogeneity in real power grids. Having established that heterogeneous β_+ can improve stability over the homogeneous β_- for a small example system, we now show that this result extends to much larger, real-world power grids. Specifically, we study the 48-generator NPCC portion of the North American power grid and the 69-generator German portion of the European power grid. Assessing the stability against small perturbations based on Eqs. (1)–(3) has the advantage of reducing the complexity of these systems to a single matrix P and its eigenvalues. For each system, we identify a local minimum β_+ that has heterogeneous β_i (and thus is distinct from β_-) and achieves the lowest λ^{\max} over 200 independent runs of simulated annealing. We find simulated annealing to be more effective than other methods in locating a minimum on a non-differentiable landscape²⁷. The resulting stability improvement over β_- is substantial: $\lambda^{\max}(\beta_-) - \lambda^{\max}(\beta_+) = 0.66$ for the NPCC network and $\lambda^{\max}(\beta_-) - \lambda^{\max}(\beta_+) = 0.42$ for the German network. The optimized β_i assignment in

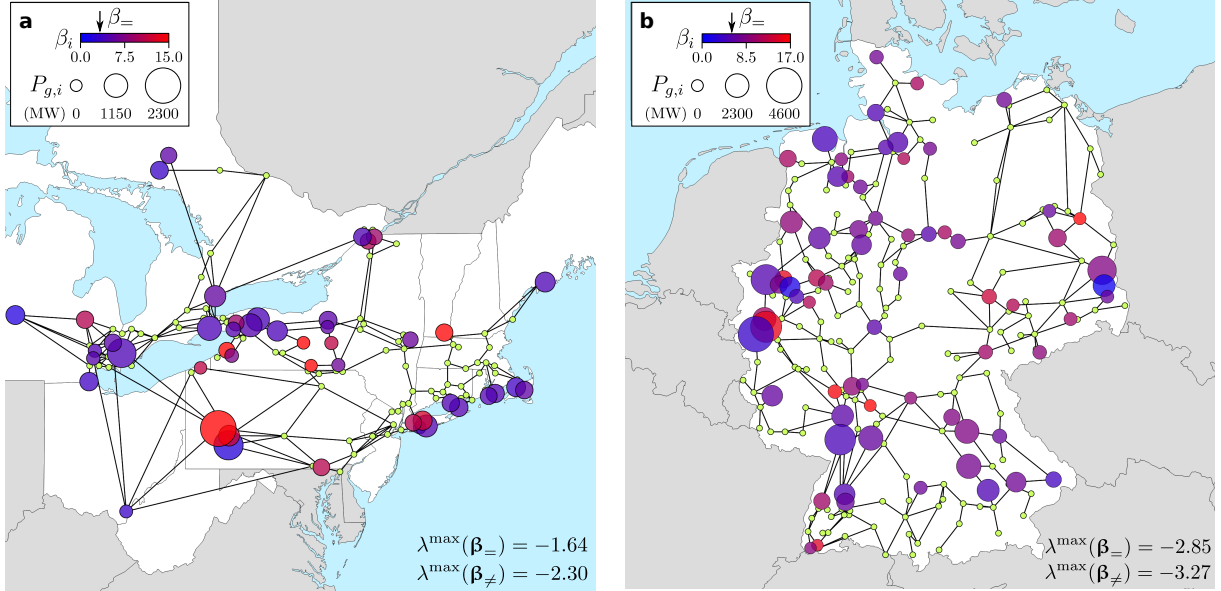


Fig. 3: Heterogeneity of optimized generator parameters β_i for two power grids. **a** Portion of the North American power grid corresponding to the former Northeast Power Coordinating Council (NPCC) region. **b** German portion of the European power grid. In both panels, a color-coded circle represents a generator or an aggregate of generators (see Methods for the aggregation procedure used), with the color indicating the corresponding optimal β_i in the vector β_{\neq} . The arrows above the color bars indicate $\beta_=$, the optimal uniform value of β_i . The λ^{\max} values for the uniform and non-uniform optimal β_i (in the vectors $\beta_=$ and β_{\neq} , respectively) are indicated at the bottom of each panel. The radius of the circle is proportional to the real power output of the generator in megawatts (MW). Small green dots indicate non-generator nodes. Details on these systems, including data sources, can be found in Methods.

β_{\neq} exhibits substantial heterogeneity across each network and also across the corresponding geographical area (Fig. 3).

To validate the prevalence of such stability-enhancing heterogeneity, we also analyze λ^{\max} as a function of *system stress level* (to be precisely defined below) for four different systems, including the two used in Fig. 3 (see Methods for detailed descriptions of the systems and data sources). To increase or decrease the level of stress in a given system, we scale the power output of all generators and the power demand at all nodes by a common constant factor. We then recompute the power flows across the entire network and the parameters of Eq. (1). The system stress level is then defined to be the common scaling factor used in this procedure. Thus, a stress level of 1 for a given system corresponds to the original demand level in the corresponding dataset. For each stress level, we estimate λ^{\max} at $\beta = \beta_{\neq}$ from 200 independent simulated